Transmission Electron Microscopy

Part IV: Electron Optics

Christoph T. Koch

Max Planck Institut für Metallforschung

Websites: hrem.mpi-stuttgart.mpg.de/koch/Vorlesung/
hrem.mpi-stuttgart.mpg.de/koch/MatlabScripts/

Electrons in electric and magnetic fields

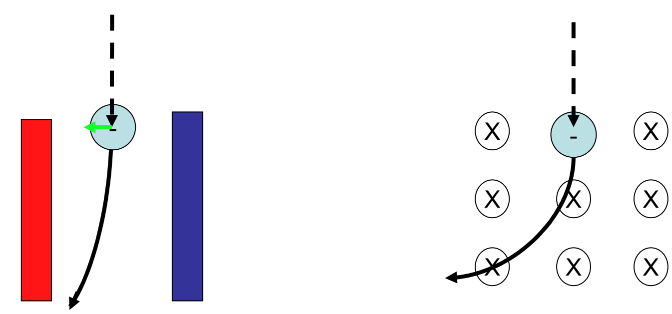

Electrostatic force | Lorentz force

$\mathbf{F}=q\mathbf{E}$ | $\mathbf{F}=q\mathbf{v}\otimes\mathbf{B}$

Since Electrons in a TEM are very fast, electron deflection using **magnetic fields** is much more efficient.
Side benefit: Only the fast electrons are affected by magnetic electron optics (no polarized dirt, etc.).

Magnetic Electron Optical Elements in a TEM

Dipole

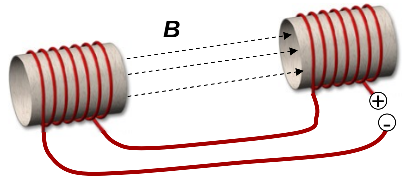

(used for deflecting the beam)

Quadrupole

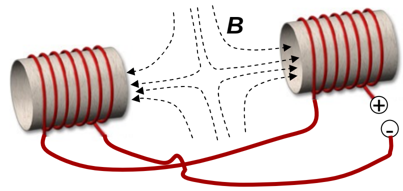

(used for compressing / stretching the beam in one direction)

Lens

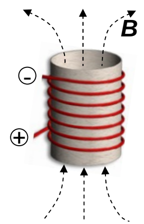

(modern electron optics also uses hexapoles, octupoles and higher order elements.)

Max-Planck Institut für Metallforschung

Universität Stuttgart

Electron Beam Deflection

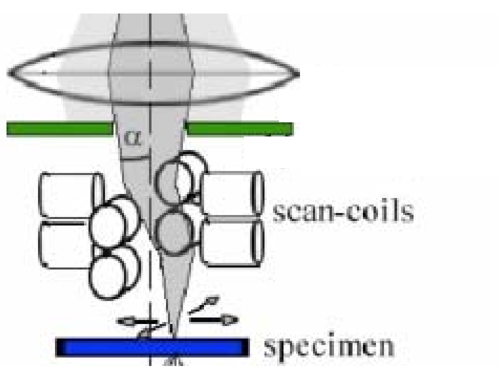

Example:
Shifting a focused beam across the specimen

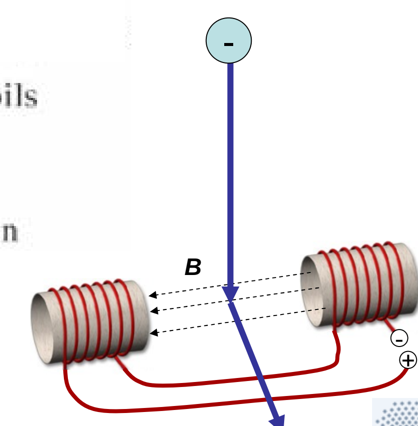

Max-Planck Institut für Metallforschung

Universität Stuttgart

Beam Shift and Beam Tilt

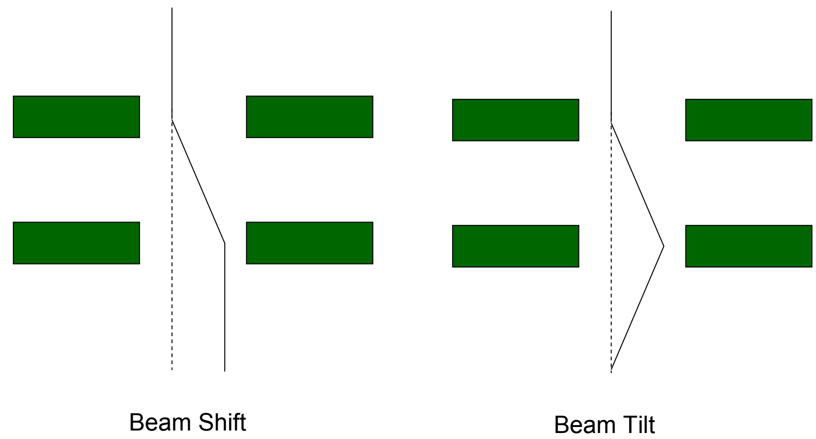

Uniaxial Stretching / Compressing of the Beam

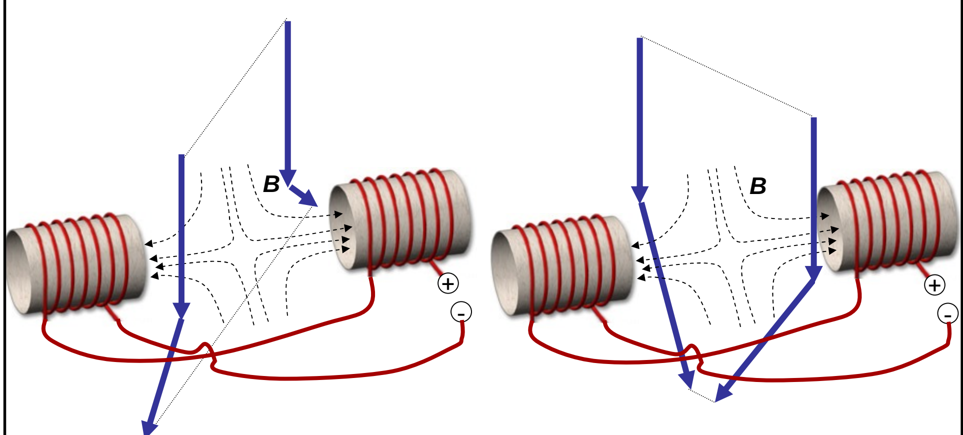

Normally, a consists of more than just one set of coils (e.g. 4).
The additional coils are used to compensate side-effects.

Focusing of Electrons by a Short Magnetic Coil

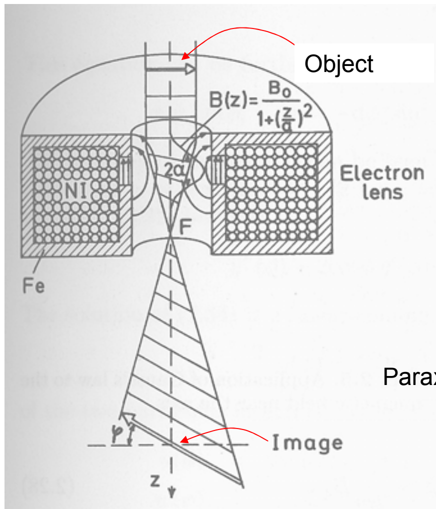

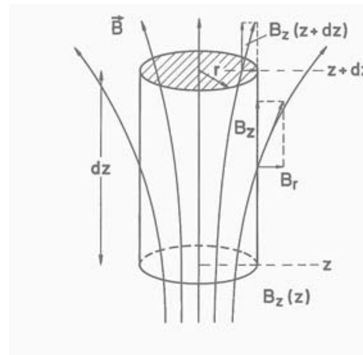

Paraxial ray equation (neglects aberrations):

$$\frac{d\vec{v}}{dz} + \frac{e}{8mV_r} B_z^2(\vec{r}) = 0$$

The Image is magnified and rotated

rel. acc. voltage

Acceleration of e⁻

Electrons travel on a Screw-like Trajectory

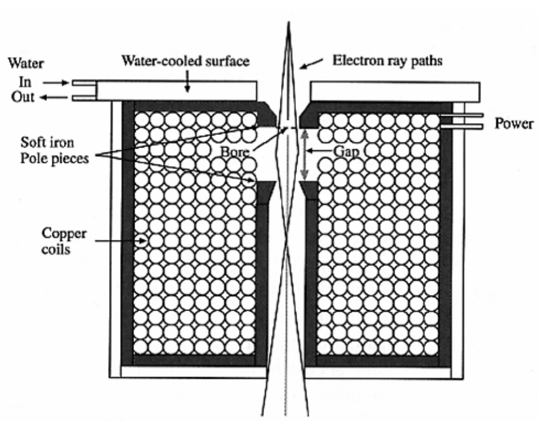

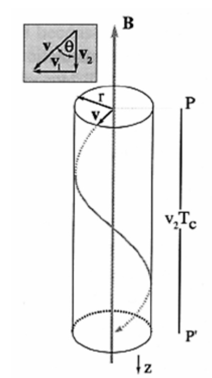

Field strength |B| ≈ 1 Tesla
(typical value in a 200 kV TEM)

Different Designs of Magnetic Lenses

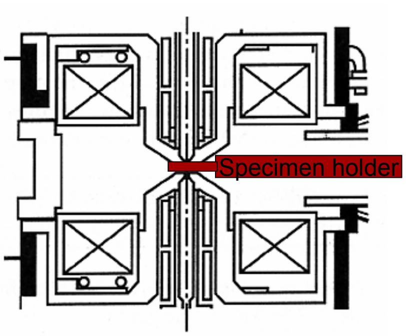

Symmetric side entry lens

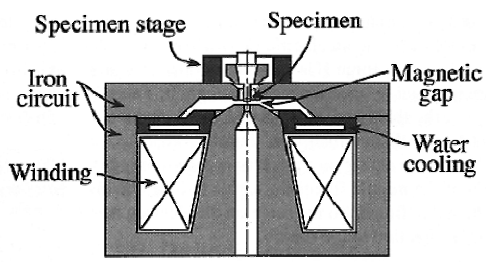

Top entry lens

Schematic of Electron Lens

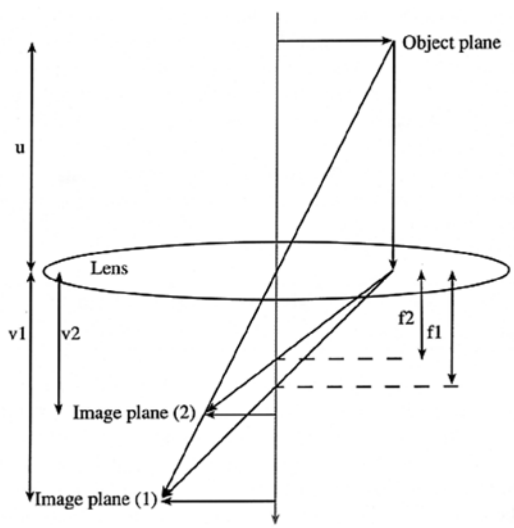

Strength of lens (its focal length f) depends on the current (and thus B(z)) in the lens.

Ray Optics: a few Definitions

meridional ray (or **tangential ray**)**:** ray in the **y**-**z** plane, where **z** points along the optic axis of the system, and **y** is perpendicular to it.

marginal ray: meridional ray touching the aperture (defines entrance- and exit pupil).

chief ray: meridional ray starting at the edge of the object, passing through the center of the aperture (defines the size of the image).

skew ray: ray that originates from an object point in the **y**-**z** plane, but does not propagate in this plane (intersects entrance pupil at some arbitrary coordinates).

sagittal ray (or **transverse ray**)**:** skew ray that intersects the pupil at *yp*=0.

paraxial ray: ray traveling near the optic axis (ray tracing: sin(θ) ≈ θ is assumed to be valid).

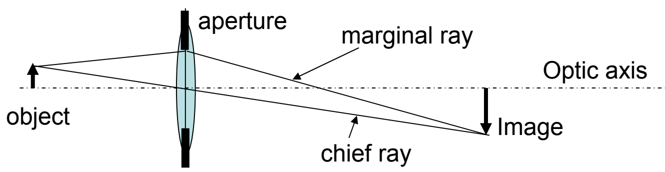

Expansion of Lens Aberrations

Imperfect lenses are treated by perturbation of the paraxial ray equation using, for example, the following expansion (other expansions of lens aberrations exist as well):

$$\chi(\vartheta,\phi) = |A_0|\vartheta\cos(\varphi-\phi_{11}) \quad \text{(image shift)}$$
$$+\frac{1}{2}|A_1|\vartheta^2\cos(2[\phi-\phi_{22}])+\frac{1}{2}|C_1|\vartheta^2 \quad \text{(astigmatism + defocus)}$$
$$+\frac{1}{3}|A_2|\vartheta^3\cos(3[\phi-\phi_{33}])+\frac{1}{3}|B_2|\vartheta^3\cos(\varphi-\varphi_{31}) \quad \text{(3-fold astigmatism + coma)}$$
$$+\frac{1}{4}|A_3|\vartheta^4\cos(4[\phi-\phi_{44}])+\frac{1}{4}|S_3|\vartheta^4\cos(2[\varphi-\varphi_{42}])+\frac{1}{4}|C_3|\vartheta^4 \quad \text{(..+..+ spherical aberration)}$$
$$+\frac{1}{5}|A_4|\vartheta^5\cos(5[\phi-\phi_{55}])+\frac{1}{5}|D_4|\vartheta^5\cos(3[\varphi-\varphi_{53}])+\frac{1}{5}|B_4|\vartheta^5\cos(\varphi-\varphi_{51})$$
$$+\frac{1}{6}|A_5|\vartheta^6\cos(6[\phi-\phi_{66}])+ \quad \ldots \quad +\frac{1}{6}|C_5|\vartheta^6$$

With increasing image resolution, higher-order aberration coefficients become important.

The spherically symmetric aberrations (C_3, C_5, …) are present even in perfect (round) lenses. Special correcting elements must therefore be designed to correct for them.

$$\vartheta = \sin^{-1}(|q|\lambda) \approx |q|\lambda \qquad \varphi = \tan^{-1}(q_y / q_x)$$

Role of Objective Aperture

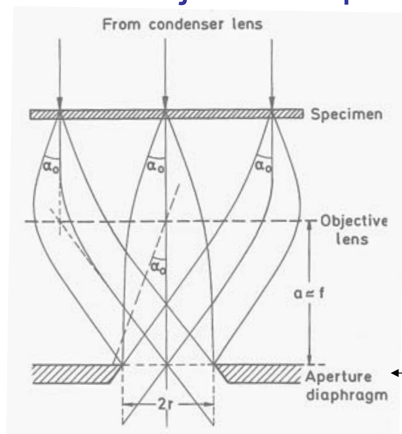

Objective aperture

The objective lens limits the range of scattering angle θ that is being transmitted by the objective lens. This limits the effect of aberrations on the image.

The objective aperture is also commonly used to produce images using only certain crystal reflections.

Image shift

Aberration (or phase distortion) function:

$$\chi(\vartheta,\phi) = |A_0|\,\vartheta\cos(\varphi - \phi_{11})$$

$$\Psi_{shifted}(\vec{r}) = \Psi(\vec{r} + \Delta\vec{r})$$
$$= \Psi_0(\vec{r}) \otimes FT^{-1}\left[\exp\left(-\frac{2\pi i}{\lambda}\chi(q,\Delta r)\right)\right]$$
$$= \Psi_0(\vec{r}) \otimes FT^{-1}\left[\exp\left(-2\pi i\vec{q}\cdot\Delta\vec{r}\right)\right]$$

Max-Planck Institut für Metallforschung Universität Stuttgart

Defocus: Huygen's Principle

"Every point on a primary wavefront serves as the source of spherical secondary wavelets, such that the primary wavefront at some later time is the envelope of these wavelets."

[“Jede Stelle einer Welle ist die Quelle einer (Kugel-) Welle”]

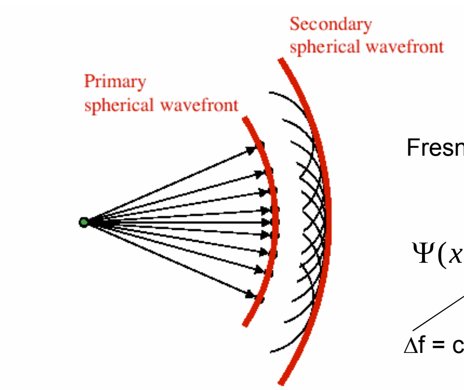

Fresnel propagation of electrons through vacuum:

$$\Psi(x, y, \Delta f) = \Psi(x, y) \otimes \exp\left(-\frac{i\pi\left[x^2 + y^2\right]}{\lambda \Delta f}\right)$$

Δf = change in focal length of objective lens

Defocus = Distance from Actual Image Plane

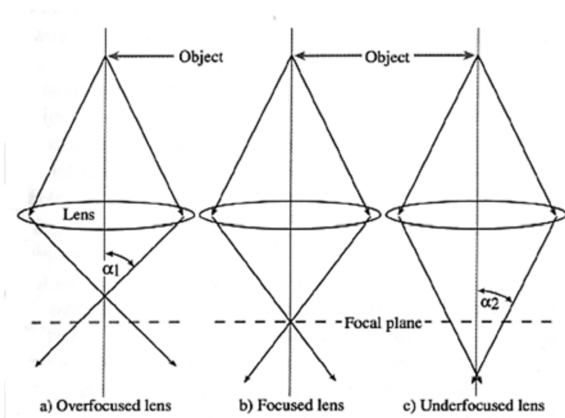

Detector or object plane of next lens

The defocus may be adjusted by changing the current running the lens

Defocus = Phase Shift

Aberration (or “phase distortion”) function: $\chi(\vartheta) = \frac{1}{2}|C_1|\vartheta^2$

$$\Psi_{shifted}(\vec{r}) = \Psi_0(\vec{r}) \otimes FT^{-1}\left[\exp\left(-i\pi\lambda\Delta f|\vec{q}|^2\right)\right]$$

Fresnel propagator in real space: $P(x,y) = \exp\left(-\frac{i\pi[x^2+y^2]}{\lambda\Delta f}\right)$

Image: $I(r) = |\Psi_{aberrated}(r)|^2$

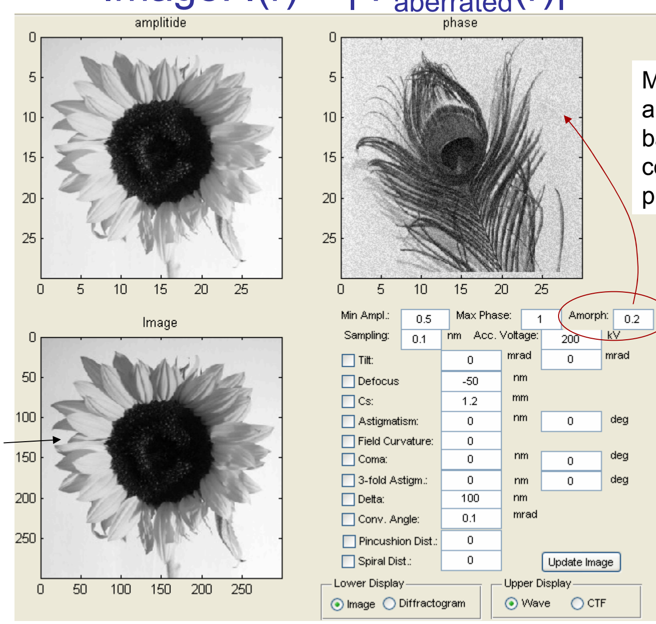

Makes amorphous background of a certain maximum phase shift

The phase of the wave function is lost in the image

Effect of Aberrations on the Image

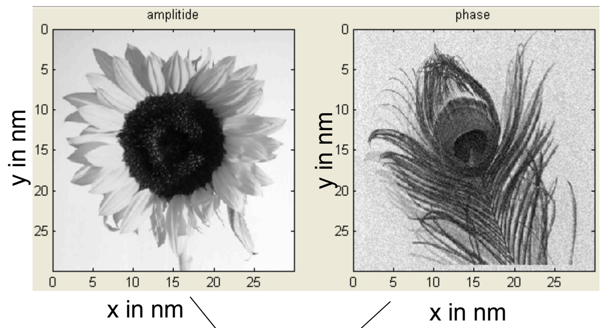

$$\Psi_{aberrated}(\vec{r}) = \Psi_0(\vec{r}) \otimes FT^{-1}\left[\exp\left(-i\chi(\vec{q})\right)\right]$$

$$\Psi_{aberrated}(\vec{q}) = \Psi_0(\vec{q})\exp\left(-i\chi(\vec{q})\right)$$

Effect of Defocus on the Image

Coherent Transfer Function (CTF)

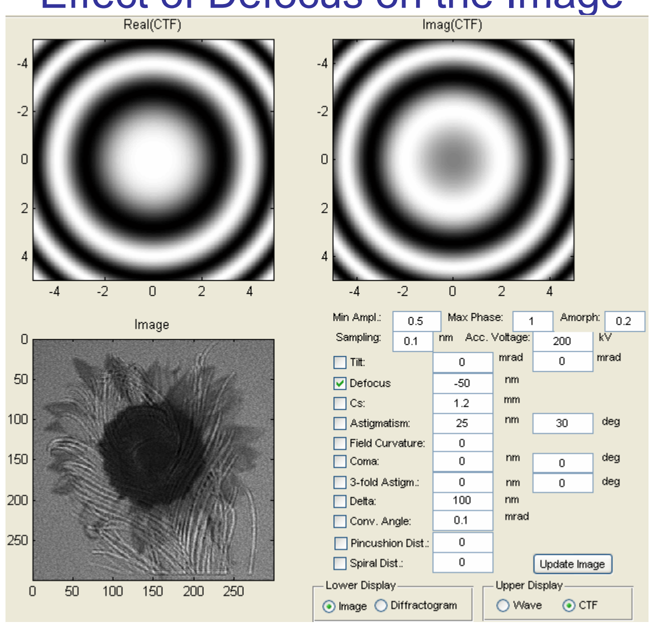

Defocused image: Mixing of amplitude and phase

Astigmatism

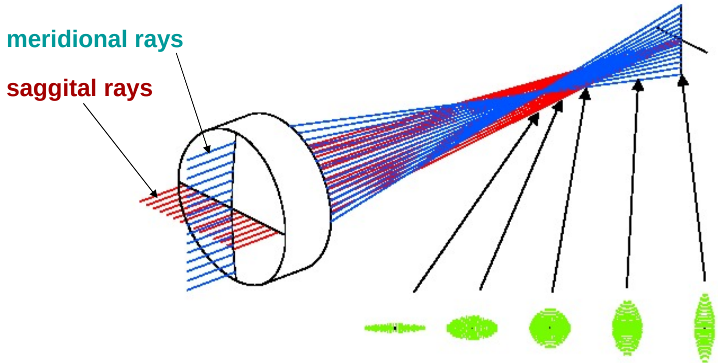

Electrons passing at different directions away from the optic axis have different focal lengths.

Aberration (or "phase distortion") function: $\chi(\vartheta,\varphi) = \frac{1}{2}|A_1|\vartheta^2 \cos(2[\varphi - \varphi_{22}])$

Correction of Astigmatism

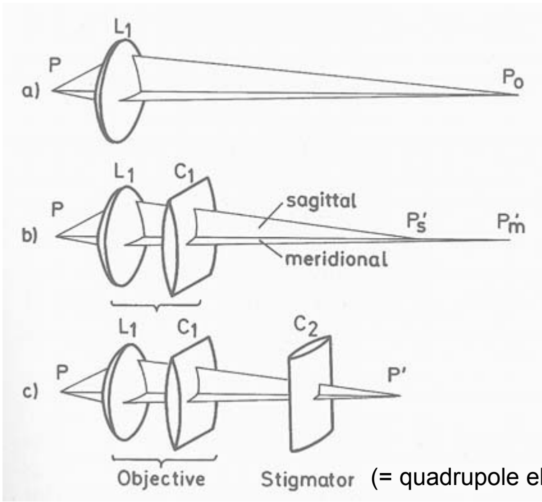

(= quadrupole element)

Effect of Astigmatism

Defocus is **small** or **large**, depending on direction

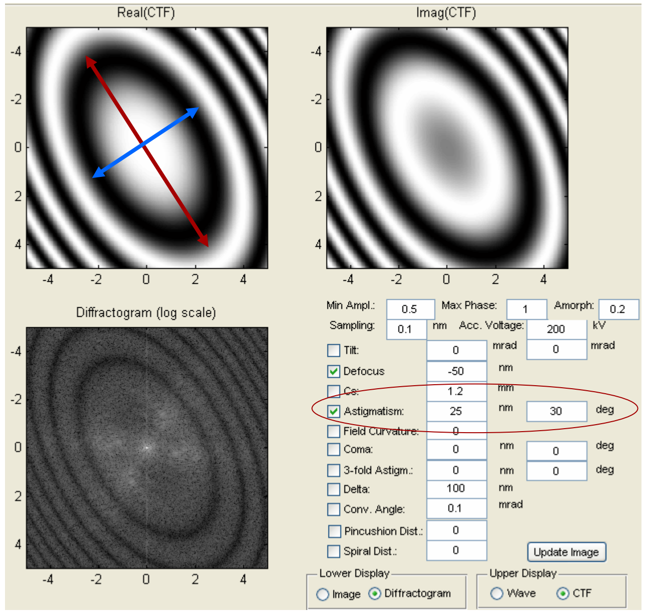

Diffractogram
= FFT of image
I(q)= FFT[I(r)]

For thin amorphous specimen:
I(q)=|Imag(CTF(q))|^2

Astigmatism

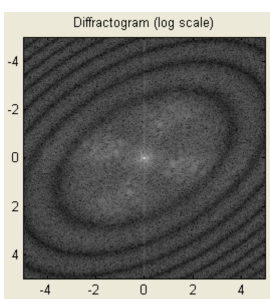

Δf=50nm, $|A_1|$=25nm

ϕ_{22}=30°

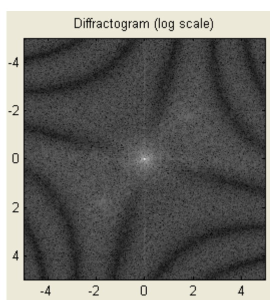

Δf=0nm, $|A_1|$=25nm

ϕ_{22}=30°

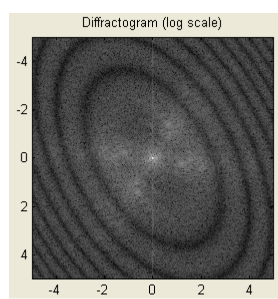

Δf=-50nm, $|A_1|$=25nm

ϕ_{22}=30°

Spherical Aberration

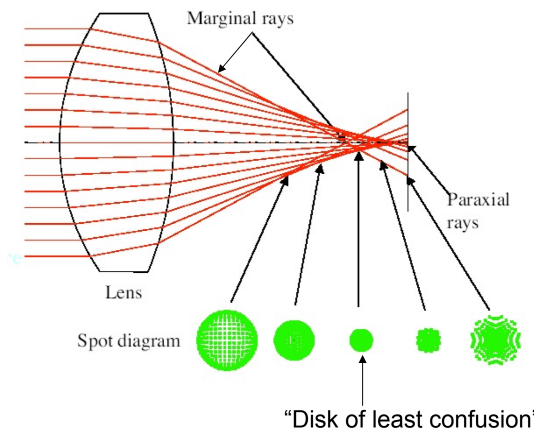

Aberration (or “phase distortion”) function: $\chi(\vartheta) = \frac{1}{4}|C_3|\vartheta^4$

Max-Planck Institut für Metallforschung Universität Stuttgart

Effect of Spherical Aberration

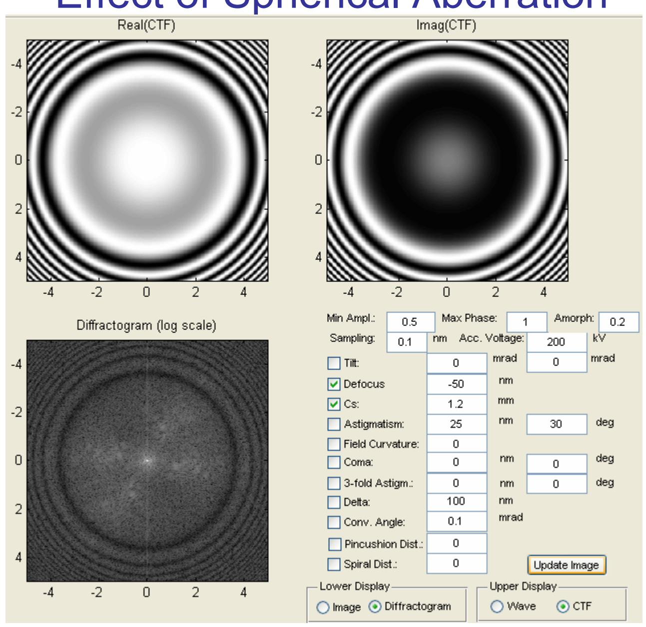

Max-Planck Institut für Metallforschung Universität Stuttgart

Effect of Spherical Aberration

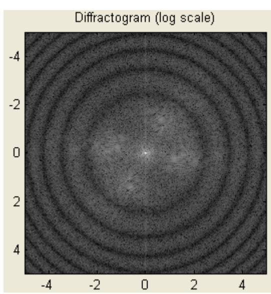

Cs = 0, Δf = -65.7nm

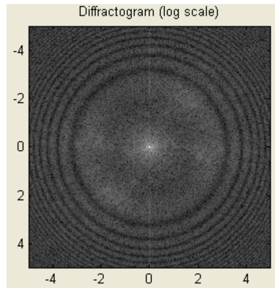

Cs = 1.2mm, Δf = 0

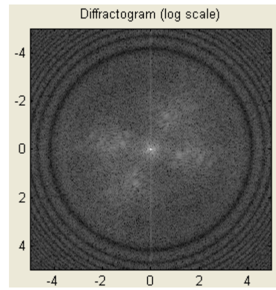

Cs = 1.2mm, Δf = -65.7nm

For a given spherical aberration C_s there is a defocus, which may optimize the transfer function for a given purpose.
The most important (and commonly used) is the **Scherzer-Focus**:

$$\Delta f_{Scherzer} = -1.2\sqrt{C_s \lambda}$$

C_s, Astigmatism and Defocus

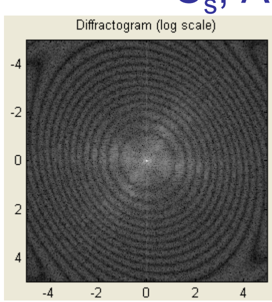

Δf=-300nm, $|A_1|$=25nm, Cs=1.2mm

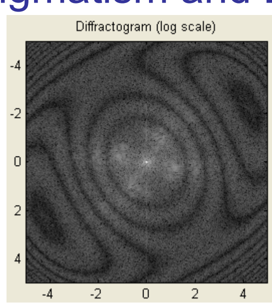

Δf=-150nm, $|A_1|$=25nm, Cs=1.2mm

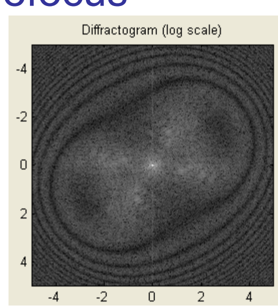

Δf=-50nm, $|A_1|$=25nm, Cs=1.2mm

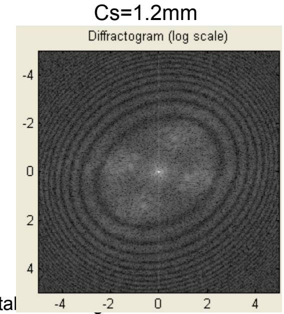

Δf=50nm, $|A_1|$=25nm, Cs=1.2mm

C_s + Beam Tilt => Image Shifts with Defocus

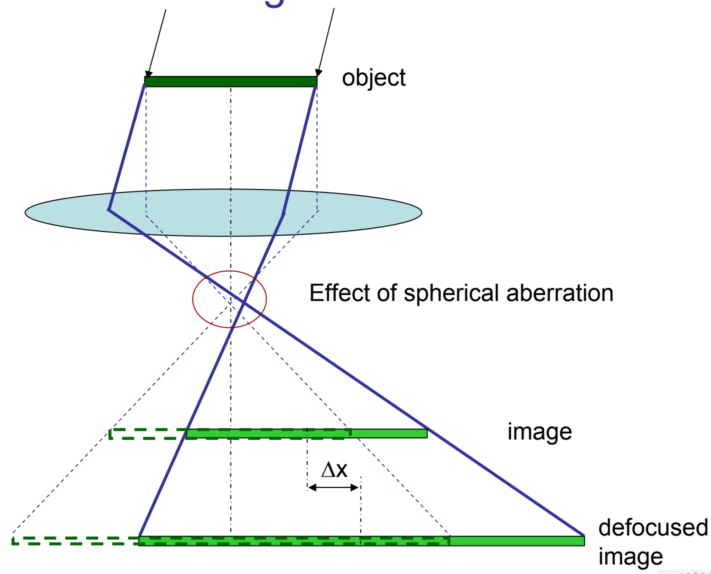

Determination of Cs

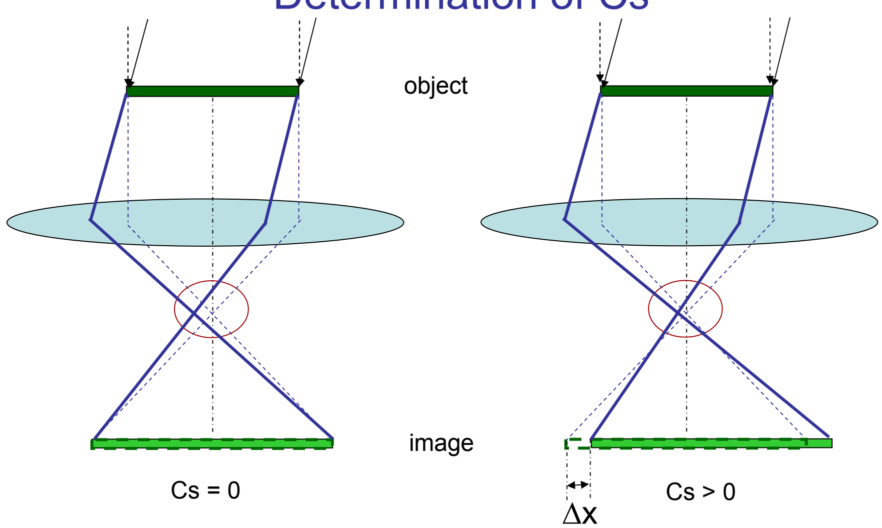

Dx: image shift
M: magnification
θ: tilt angle

$$\Delta x = MC_s\theta^3$$

Coma

Coma is defined as a variation in magnification over the entrance pupil

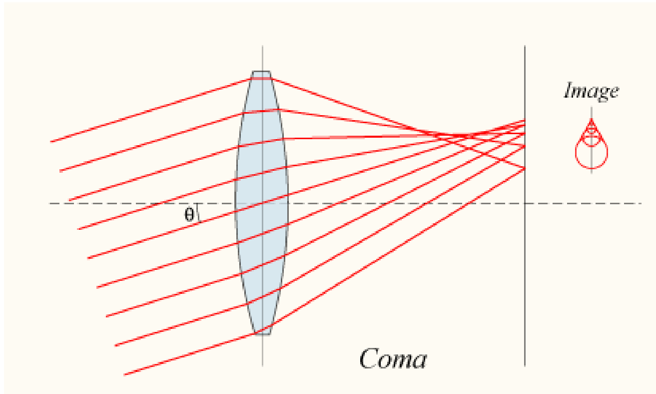

$$\chi(\vartheta,\phi) = \frac{1}{3}|B_2|\vartheta^3 \cos(\varphi - \varphi_{31})$$

Effect of Coma

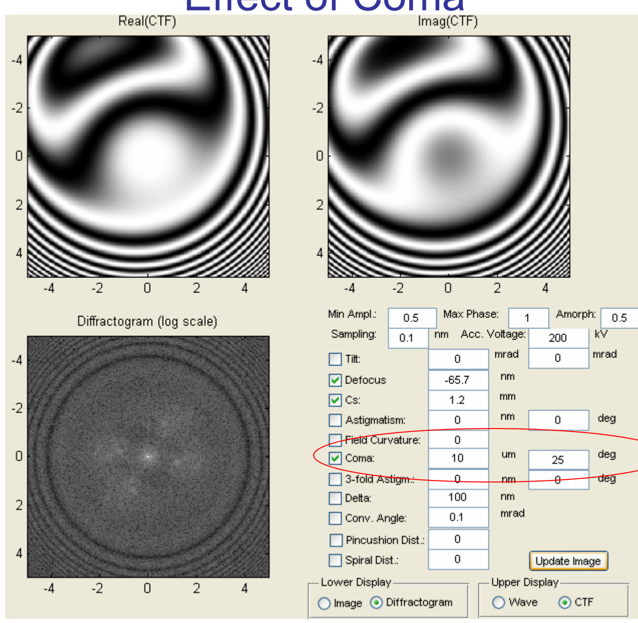

Asymmetric Aberrations only visible with Tilt

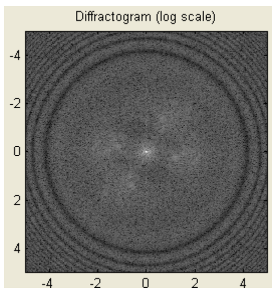

C_s = 1.2mm, Δf = -65.7nm, B_2=10µm, Tilt=(0,0)mrad

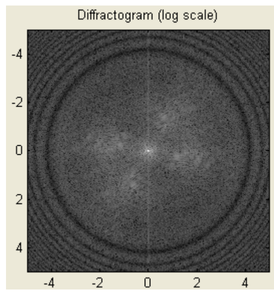

C_s = 1.2mm, Δf = -65.7nm, B_2=0µm, Tilt=(0,0)mrad

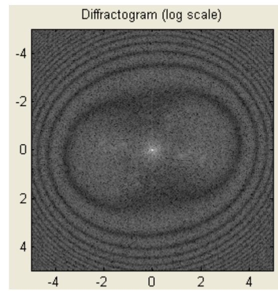

C_s = 1.2mm, Δf = -65.7nm, B_2=10µm, Tilt=(2,0)mrad

Asymmetric aberrations may reduce the contrast in the diffractogram, but do not alter its shape.

Coma and **tilt** may appear as **astigmatism** in the diffractogram

Zemlin Tableau

The Zemlin tableau is a series of diffractograms recorded at different illumination tilt angles. It allows evaluation of even and odd aberrations, which is not possible without tilt.

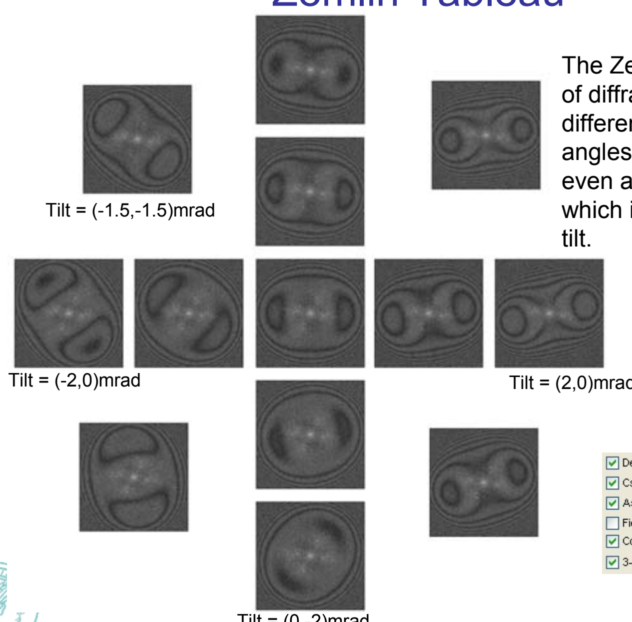

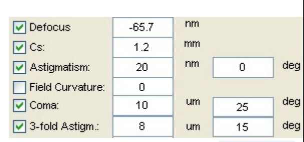

3-fold Astigmatism

$$\chi(\vartheta,\phi) = \frac{1}{3}|A_2|\vartheta^3 \cos(3[\phi - \phi_{33}])$$

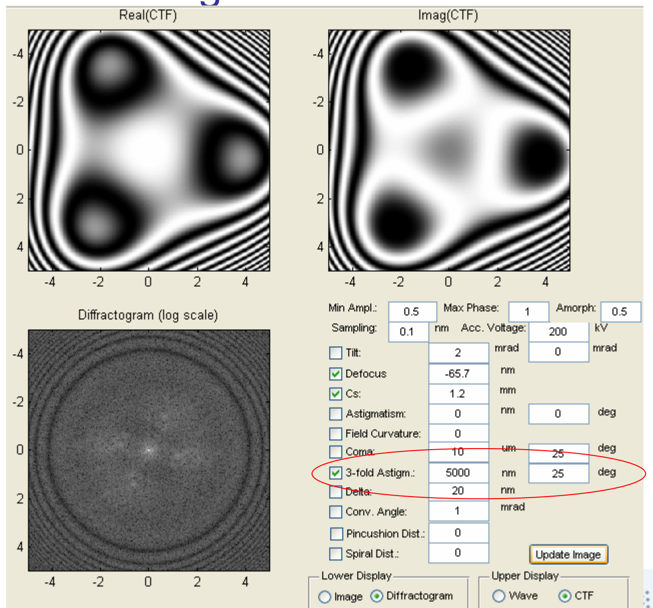

3-fold astigmatism, being an asymmetric aberration, is not visible in the geometry of the diffractogram

Field Curvature

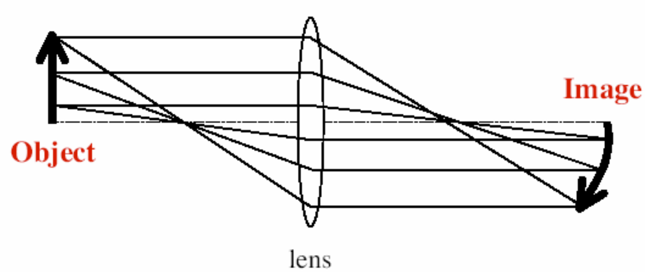

The defocus changes with distance from the optic axis (commonly neglected).

Lens distortions

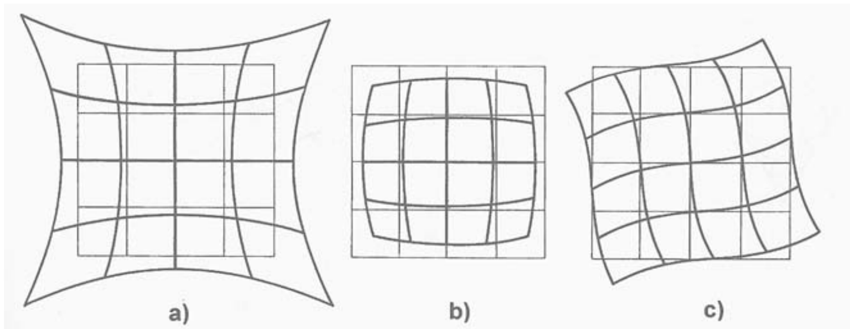

Fig. 2.15. (a) Pincushion, (b) barrel and (c) spiral distortion of a square grid

Lens distortions

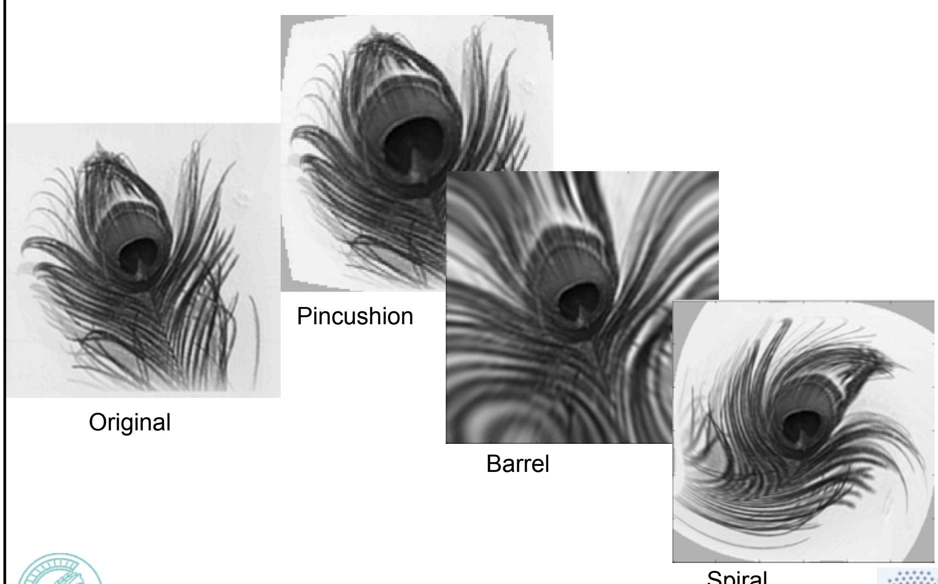

Aberrations at Low and High Magnification

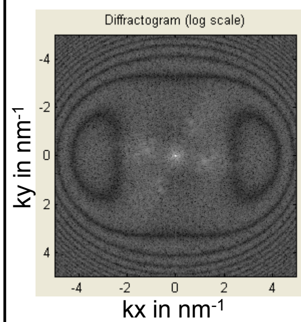

C_s = 1.2mm, Δf = -65.7nm, $|A_1|$=25nm, **dx = 1Å**

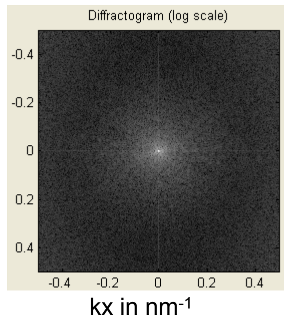

C_s = 1.2mm, Δf = -65.7nm, $|A_1|$=25nm, **dx = 1nm**

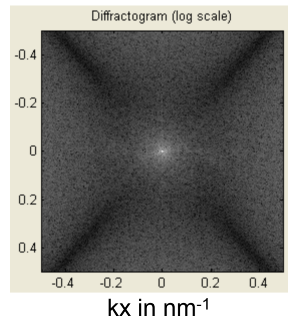

C_s = 1.2mm, Δf = -65.7nm, $|A_1|$=500nm, **dx = 1nm**

Aberrations of higher order become insignificant at lower magnification.
e.g.: Considerable amount of astigmatism produce no visible effect at lower magnification.

Phase Object Approximation (POA)

$$\Psi(\vec{r}) \approx \exp\left(-i\sigma V_p(\vec{r})\right)$$

V_p(r): projected potential of specimen (computed via the structure factor).

$$V_p(x,y) = \int V(x,y,z)dz$$

σ: electron beam interaction constant

$$\sigma = 2\pi me\lambda / h^2$$

Weak Phase Object Approximation (WPOA)

For very thin specimen consisting of light elements (e.g. biological samples), the phase object approximation may be approximated again by the weak phase object approximation:

$$\Psi(\vec{r}) \approx \exp\left(-i\sigma V_p(\vec{r})\right) \approx 1 - i\sigma V_p(\vec{r})$$

Linear Imaging and the WPOA

$$\begin{aligned} I(\vec{r}) &= \left|\Psi_{aberrated}(\vec{r})\right|^2 \\ &\approx \left|\left[1 - i\sigma V_p(\vec{r})\right] \otimes FT^{-1}\left[\exp\left(-i\chi(\vec{q})\right)\right]\right|^2 \\ &= \left|FT^{-1}\left[\exp\left(-i\chi(\vec{q})\right)\right] - i\sigma V_p(\vec{r}) \otimes FT^{-1}\left[\exp\left(-i\chi(\vec{q})\right)\right]\right|^2 \\ &\approx 1 - 2\sigma V_p(\vec{r}) \otimes \mathrm{Im}\left\{FT^{-1}\left[\exp\left(-i\chi(\vec{q})\right)\right]\right\} + \ldots \end{aligned}$$

In the WPOA the image contrast is the convolution of the projected potential with the imaginary part of the CTF.

This first approximation to the image contrast is often called linear imaging, since only interference between the central beam and scattered beam is considered.

Nonlinear Imaging

$$I(\vec{r}) = \left|\Psi_{aberrated}(\vec{r})\right|^2$$
$$= \left|\Psi_0(\vec{r}) \otimes FT^{-1}\left[\exp(-i\chi(\vec{q}))\right]\right|^2$$

Non-linear imaging theory includes real- and imaginary part of the exit face wave function, as well as all the terms neglected in the approximation used for linear imaging (see previous slide).

Partial Coherence

While coherent aberrations mingle amplitude and phase information in the images, partial coherence destroys information within the image all together.

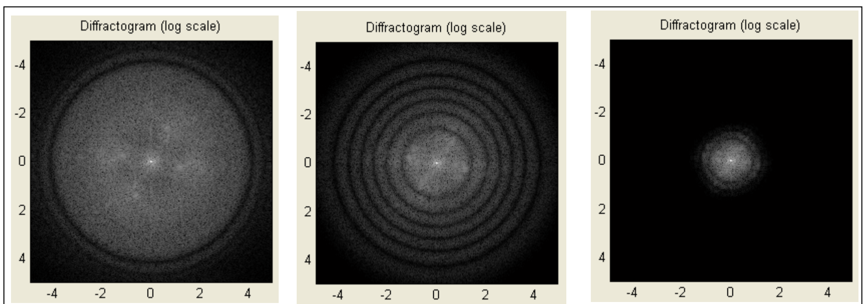

C_s = 1.2mm, Δf = -65.7nm, Δ=20nm, α=1mrad | C_s = 1.2mm, Δf = -200nm, Δ=20nm, α=1mrad | C_s = 1.2mm, Δf = -500nm, **Δ=20nm**, **α=1mrad**

Finite values of Δ and α are a result of limited (partial) **temporal (longitudinal)** and **spatial (transversal)** coherence as well as chromatic aberrations.

(A closer look at electron sources is required prior to further discussion of partial coherence)

Electron Gun design

Filament heating:
-Helps electrons to overcome the work function of the filament material.

Wehnelt cylinder:
- At a lower potential than the filament.
- Suppresses extraction of electrons from side of filament.

Anode:
-The Anode serves to extract accelerate electrons to < 7keV.
- The high tension is applied after electrons have left the gun.

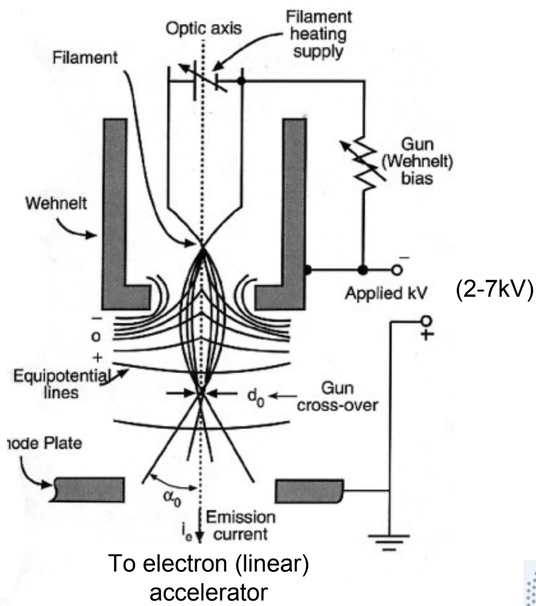

Extracting Electrons using a Wehnelt Grid

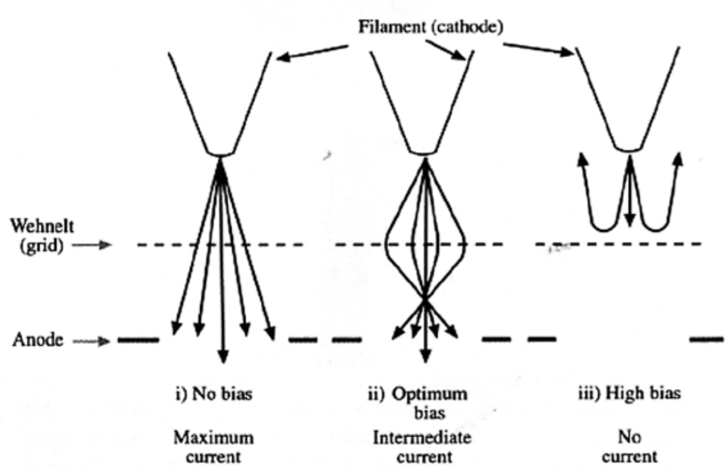

The Wehnelt grid rejects electrons below a certain kinetic energy. Since electrons from the tip of the filament have the highest kinetic energy, they may be selected by using the proper bias voltage.

Effect of Extraction Voltage (Wehnelt Bias)

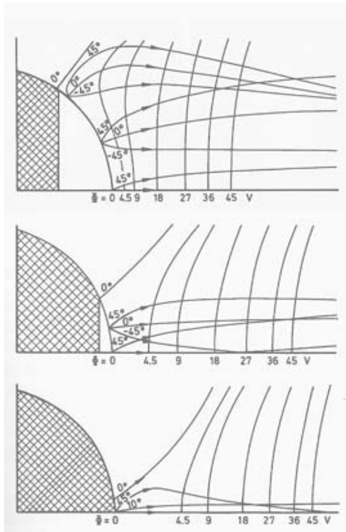

A higher extraction voltage or lower Wehnelt Bias) produces a larger field at the filament tip, but it also increases the area from which electrons are contributing to the beam.

If the field at the filament tip is too low, only very few electrons are sucked into the beam.

Thermionic Gun (W – tip)

SEM image of W-tip

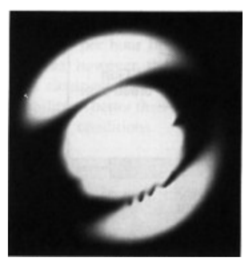

Low heating current

Normal heating current

Image of Tip
(No specimen, detector plane conjugate to electron source)

Brightness

Definition Brightness: $\beta = \frac{j}{\pi \vartheta^2}$

j : max. achievable current density
θ: size of aperture (semi-angle)

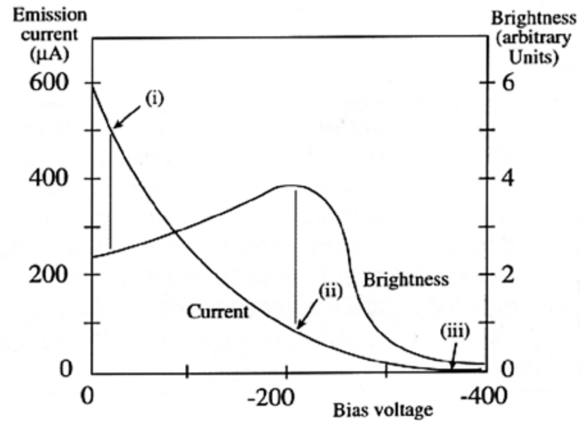

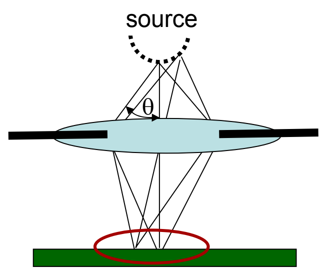

Current density limited by tip size.

([i], [ii], [iii] correspond to diagrams on previous slide)

Brightness

The theoretical upper limit for the brightness is usually given as:

$$\beta_m = \frac{\rho e V_r}{\pi k T}$$

ρ: Emission current density at the filament (ρ ~ exp(cT))
V_r:Accelerating voltage (relativistically corrected)
k: Boltzmann's constant
T: Temperature

This means that higher accelerating voltage gives also a higher brightness

Max-Planck Institut für Metallforschung Universität Stuttgart

Effect of Partial Spatial Coherence

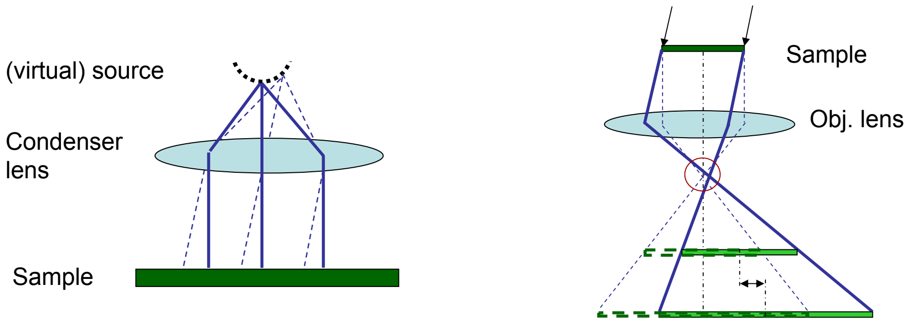

The presence of aberrations (e.g. defocus, C_s) causes the bright-field image to shift with a change in beam tilt. Superimposing several images of different beam tilt will produce a blurred image.

Relevant Virtual Source Size

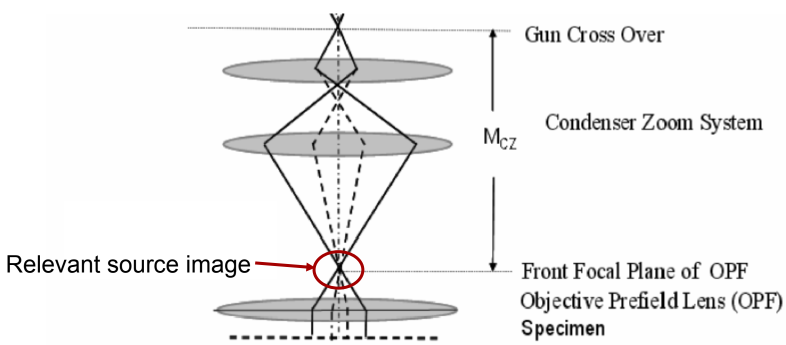

The cross over in the front focal plane is commonly a demagnified image of the gun cross over.

The spatial incoherence effects depend on the size of the cross over in front of the objective pre-field lens.

Thermionic Gun (LaB_6)

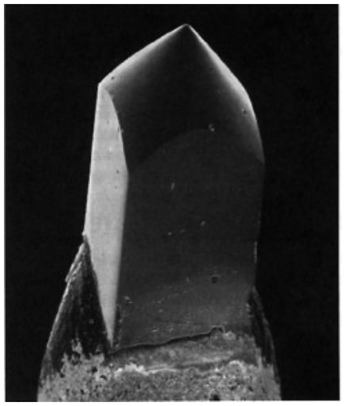

SEM image of a LaB_6-tip

Low heating current

Normal heating current

Image of LaB_6 electron source

Thermionic vs. Field-Emission Gun

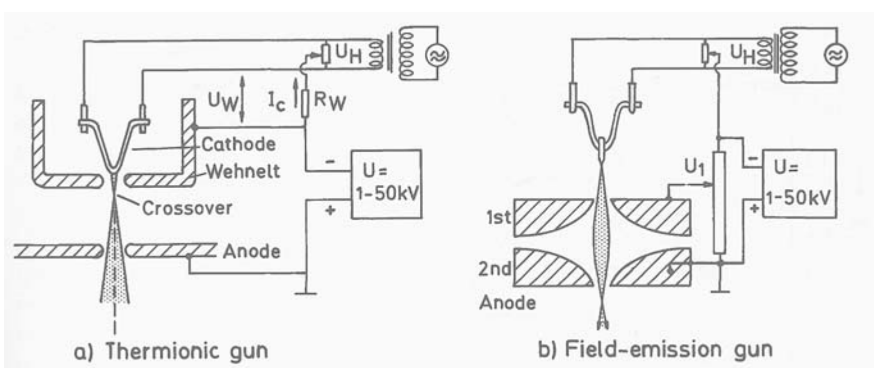

In a field emission gun the electrons not already excited to outside the tip
but they are extracted by a large electric field
(E is inversely proportional to the tip radius).

Max-Planck Institut für Metallforschung
Universität Stuttgart

Field Emission Gun (FEG)

Electrons are extracted by the electric field t the tip. In Schottky FEGs the work function is lowered by:

1. Coated the tip with LaB6
2. Heating to about 1800°C

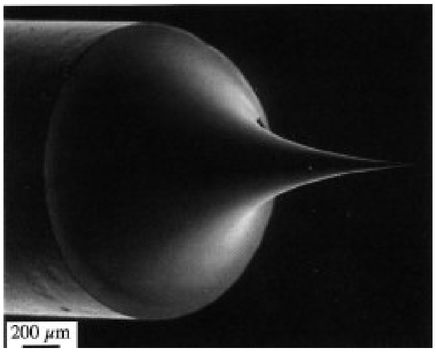

SEM image of a FEG-tip

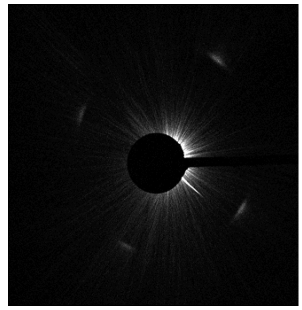

Emission image of a Schottky emitter (central spot has been blocked – the tip is a single crystal)

E = V/r

E: Electric field at tip surface
V: Applied extraction voltage
r: Radius of tip

Comparison of Electron Sources

Z-dependent work function offset produced by the high electrostatic field at filament tip

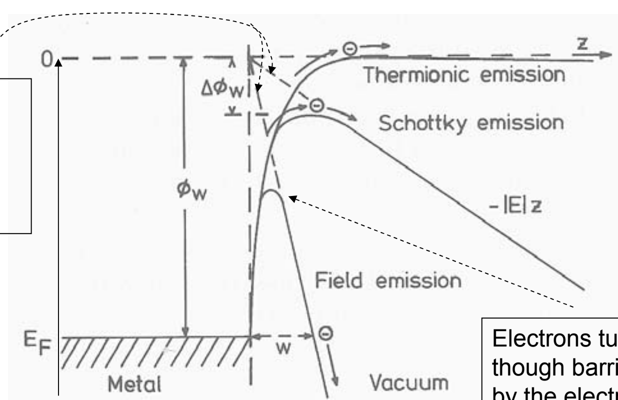

Electrons tunnel though barrier thinned by the electric field

energy

Thermionic emission: Electrons must overcome Fw by thermal excitation only
Field emission: A high electric field lowers the work function at already small distances away from the surface -> electrons may tunnel through the remaining barrier.

Comparison of Electron Sources

	W	Lab6	Schottky-FEG	Cold-FEG
Work function *f*	4.5 eV	2.4 eV	2.8eV	4.5 eV
Temperature *T*	2700 K	1700 K	1800K	300 K
Current density j_c	1-3 A/cm^2	20-50 A/cm^2	500 A/cm^2	$10^5 10^6$ A/cm^2
Crossover ∅	50 µm	10 µm	≈ 10nm	≈ 2.5nm
Brightness	10^5 A/m^2/sr	10^6 A/cm^2/sr	10^8 A/cm^2/sr	10^9 A/cm^2/sr
Energy Width	3 eV	1,5 eV	0.7eV	0,3 eV
Current stability	< 1 %/h	< 1 %/h	< 1 %/h	5 %/h
Vacuum	10^{-2} Pa	10^{-4} Pa	10^{-6} Pa	10^{-8} Pa
Life time	100 h	500 h	> 1000 h	> 1000 h

Experimental defocus series

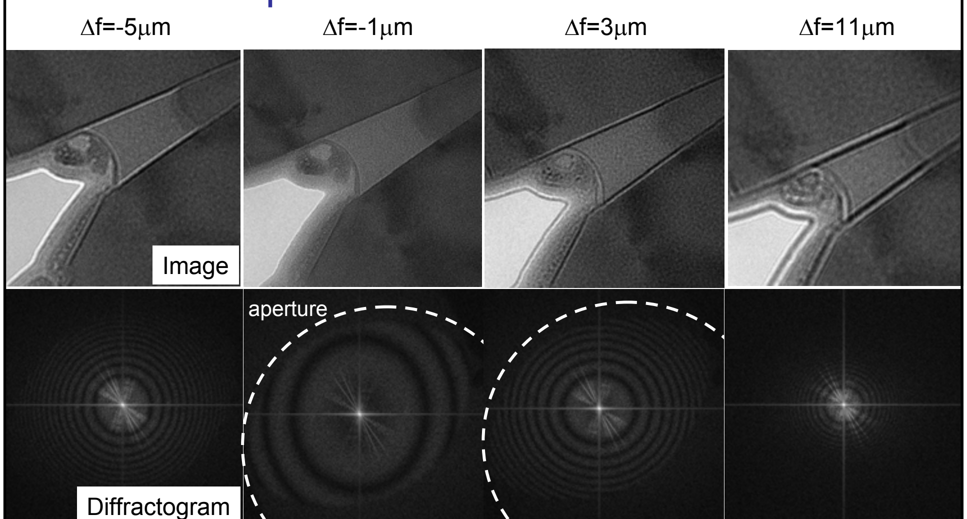

Sample: Amorphous pocket in a $SrTiO_3$ ceramic
Electron source: Field Emission Gun (FEG)

Temporal Partial Coherence

$$I(\vec{r}) = \left|\Psi_{aberrated}(\vec{r})\right|^2$$
$$= \int_{E-\Delta E}^{E+\Delta E} f(E')\left|\Psi_0(\vec{r}) \otimes FT^{-1}\left[\exp\left(-i\chi(\vec{q}, \Delta f\left[E'\right])\right)\right]\right|^2 dE'$$

A finite spread of energy of the electrons traversing the optical system of the microscope reduces the temporal (or longitudinal) coherence of the electron wave package. (Heisenberg's uncertainty principle dE*dt>h/2)

Chromatic Aberration

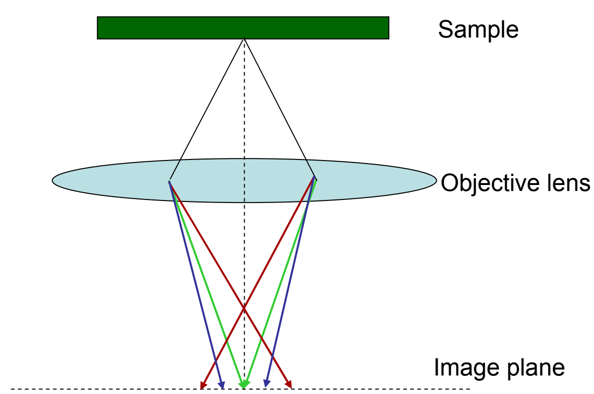

Electrons of different wavelength are being focused in different planes. The chromatic aberration defines how much the focus of the objective lens depends on the wavelength. If the Electron beam is not perfectly monochromatic, this will limit the resolution of an image.

Max-Planck Institut für Metallforschung Universität Stuttgart

Chromatic Aberration and Defocus Spread

The presence of electrons with different energies, as well as microscope instabilities produce images that are actually a superposition of images with defoci varying within a range of Δ_f:

$$\Delta_f = C_c \sqrt{\left(\frac{\sigma(E)}{E}\right)^2 + \left(\frac{2\sigma(I)}{I}\right)^2}$$

σ(..): standard deviation of this variable
E: energy of incident electrons (produced by high voltage instability and energy spread of electrons leaving the filament)
I: current in the objective lens

Spatial Partial Coherence

$$I(\vec{r}) = \left|\Psi_{aberrated}(\vec{r})\right|^2$$
$$= \int_{k_x-\Delta k_x}^{k_x+\Delta k_x} \int_{k_y-\Delta k_y}^{k_y+\Delta k_y} f(\vec{k}')\left|\Psi_0(\vec{r},\vec{k}') \otimes FT^{-1}\left[\exp\left(-i\chi(\vec{q},\vec{k}')\right)\right]\right|^2 d^2\vec{k}$$

The image intensity at the detector is the (incoherent) superposition of images produced by differently inclined electron beams.

Spatial and Temporal Partial Coherence

$$I(\vec{r}) = \left|\Psi_{aberrated}(\vec{r})\right|^2$$

$$= \int_{k_x-\Delta k_x}^{k_x+\Delta k_x} \int_{k_y-\Delta k_y}^{k_y+\Delta k_y} \int_{E-\Delta E}^{E+\Delta E} f(E')f(\vec{k}')\left|\Psi_0(\vec{r},\vec{k}') \otimes FT^{-1}\left[\exp\left(-i\chi(\vec{q},\vec{k}',E')\right)\right]\right|^2 dE' d^2\vec{k}'$$

The image intensity at the detector is the (incoherent) superposition of images produced by differently inclined electron beams.

It is commonly assumed that orientation and energy spread are distributed Gaussian-like. In a commonly used approximation the transfer function is then modified by envelope functions:

$$CTF(q) = \exp(-i\chi(q)) \cdot \exp\left(-2(\pi\Delta_f)^2 \left|\frac{d\chi(q)}{d\Delta f}\right|^2\right) \cdot \exp\left(-\left(\frac{\alpha}{2\lambda}\right)^2 \left|\frac{d\chi(q)}{dq}\right|^2\right)$$

α: source spread (spread of angular distribution of incident electrons)

Effect of Envelope Functions

Temporal coherence envelope: $E_\Delta(q) = \exp\left(-2(\pi\Delta_f)^2 \left|\frac{d\chi(q)}{d\Delta f}\right|^2\right)$

This envelope is largely independent of microscope aberrations (except for chromatic aberration)

Spatial coherence envelope: $E_s(q) = \exp\left(-\left(\frac{\alpha}{2\lambda}\right)^2 \left|\frac{d\chi(q)}{dq}\right|^2\right)$

This envelope depends on all the microscope aberrations and becomes small, where the CTF is strongly oscillating. Images at different defocus may therefore contain information of different spatial frequency ranges.

More exactly: Transmission Cross Coefficient

$$I(\vec{r}) = \mathrm{FT}^{-1}\left[\int \Psi_0(\vec{q}+\vec{q}')T(\vec{q}+\vec{q}',\vec{q}')\Psi_0^*(\vec{q}')d^2\vec{q}'\right]$$

Transmission Cross Coefficient

Temporal incoherence
Spatial incoherence
Coherent transfer funcion

$$TCC(q+q',q') = T_\Delta(q+q',q')T_s(q+q',q') \times exp(-i[\chi(q+q')-\chi(q')])$$

$$T_\Delta(q+q',q') = \exp\left(-2(\pi\Delta_f)^2\left[\frac{\delta\chi(q+q')}{\delta\Delta f}-\frac{\delta\chi(q')}{\delta\Delta f}\right]^2\right)$$

$$T_s(q+q',q') = \exp\left(-\left(\frac{\alpha}{2\lambda}\right)^2\left[\frac{\delta\chi(q+q')}{\delta(q+q')}-\frac{\delta\chi(q')}{\delta q}\right]^2\right)$$

Max-Planck Institut für Metallforschung
Universität Stuttgart

Example: High-Resolution TEM

Δf = -605nm

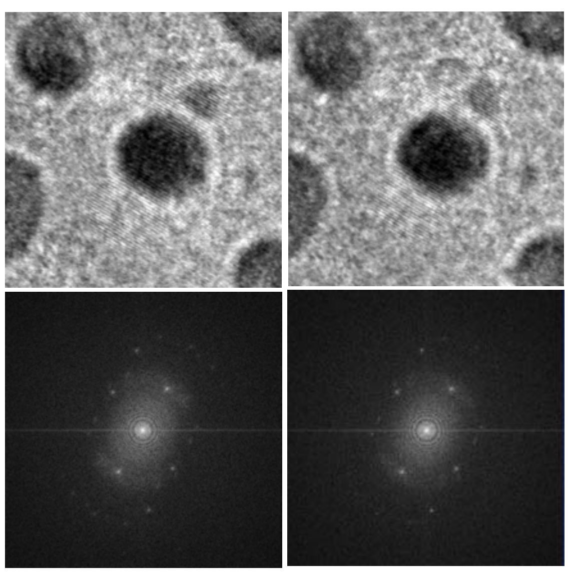

Δf = -665nm

The information transfer is highly non-linear

Max-Planck Institut für Metallforschung
Universität Stuttgart

Focal series of HRTEM images

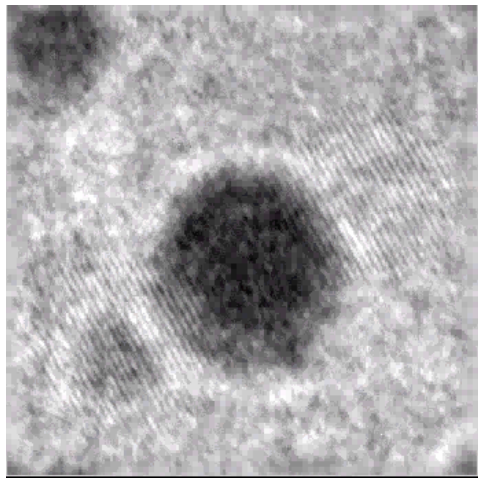

Amplitude of images of 20 image Focal series
[300kV, Δf_1=-605nm (dΔf=-3nm)]

Sample: Gold sphere on amorphous Germanium

Data kindly provided by:
Michael Pelsozy,
Frank Ernst,
Thomas Zawodzinski
Case Western Reserve University

$$|\Psi(r)| = \sqrt{I(r)}$$

(animation)

Max-Planck Institut für Metallforschung

Universität Stuttgart

Phase and Amplitude of HRTEM image

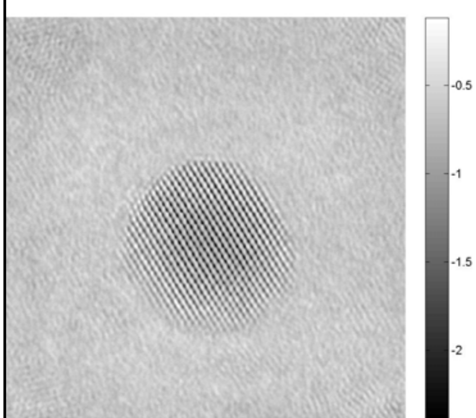

Phase

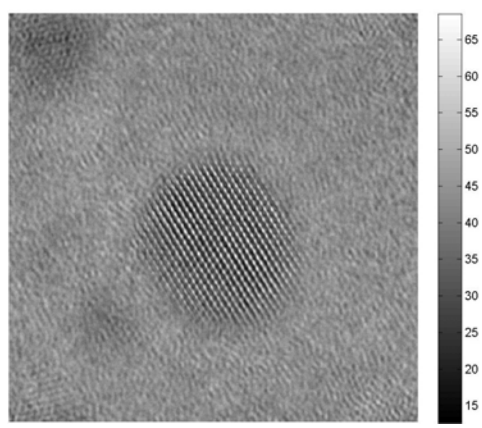

Amplitude

Phase and amplitude reconstructed from focal series of a Gold particle on a thin Carbon film.

Max-Planck Institut für Metallforschung

Universität Stuttgart